

Epitaxial and Large Area Sb₂Te₃ Thin Films on Silicon by MOCVD

Martino Rimoldi,^a Raimondo Cecchini,^a Claudia Wiemer,^a Alessio Lamperti,^a Emanuele Longo,^a
Lucia Nasi,^b Laura Lazzarini,^b Roberto Mantovan^a * and Massimo Longo^a *

^a Institute for Microelectronics and Microsystems, CNR-IMM Unit of Agrate Brianza, via C. Olivetti 2, 20864, Agrate Brianza, Italy

^b University of Milano-Bicocca, Department of Material Science, Via R. Cozzi 55, 20126, Milan, Italy

^b Institute of Materials for Electronics and Magnetism, CNR-IMEM, Parma, Parco Area delle Scienze, 7/A, 43100 Parma, Italy

* massimo.longo@mdm.imm.cnr.it

* roberto.mantovan@mdm.imm.cnr.it

Supplementary Information

Table of Contents	Page
1. SEM Images	2
2. AFM Images	3
3. TEM Images	5
4. TXRF Spectra	6
5. XP Spectra	7
6. XRR Measurements	10
7. XRD Measurements	10

1. SEM Images

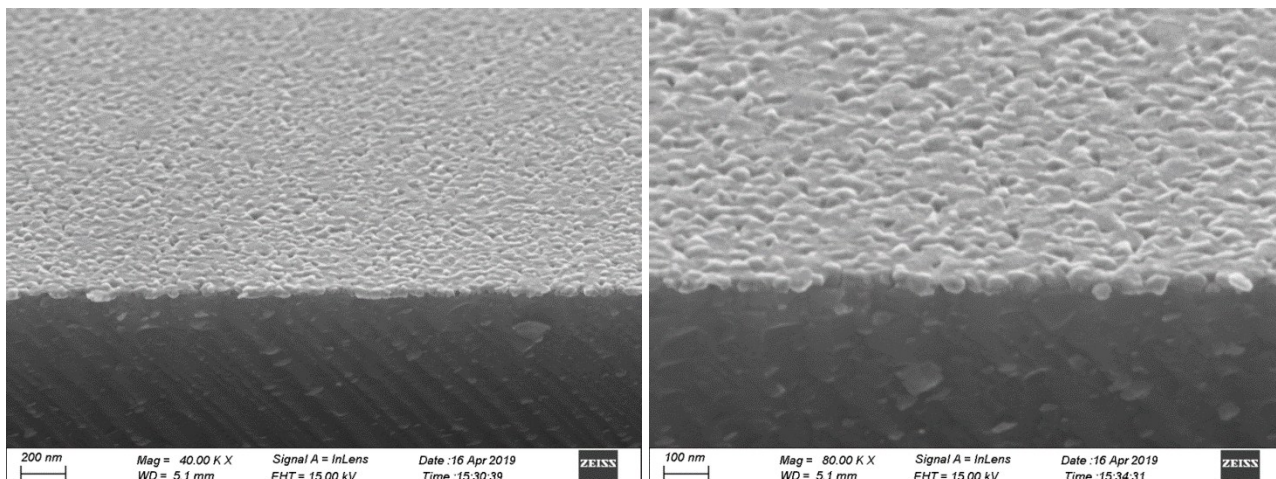


Figure S1. Tilted cross-section SEM images of Sb_2Te_3 - *As Deposited (1)* films.

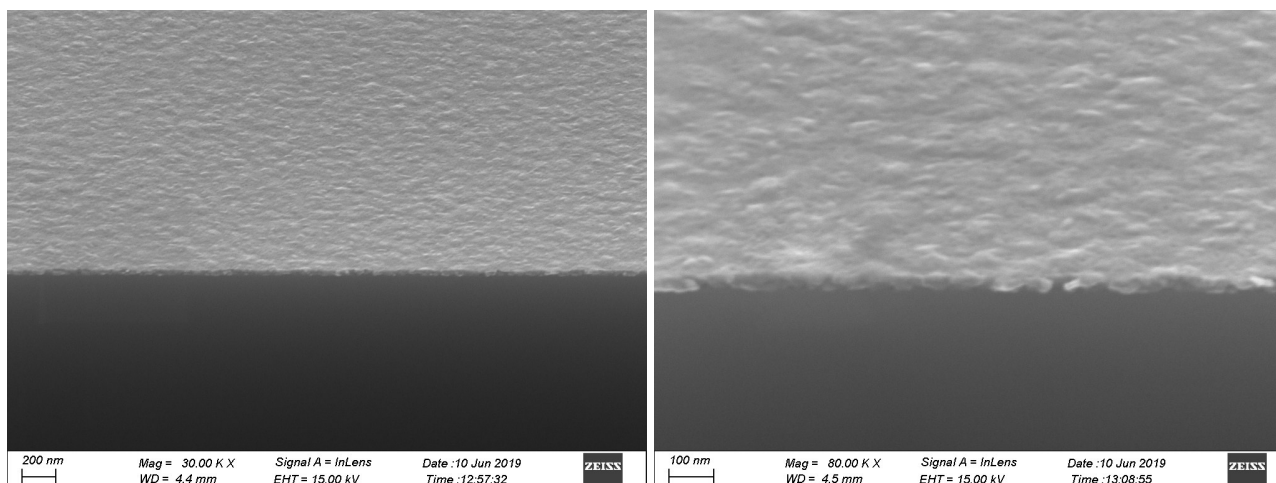


Figure S2. Tilted cross-section SEM images of Sb_2Te_3 - *Substrate Annealing (2)* films.

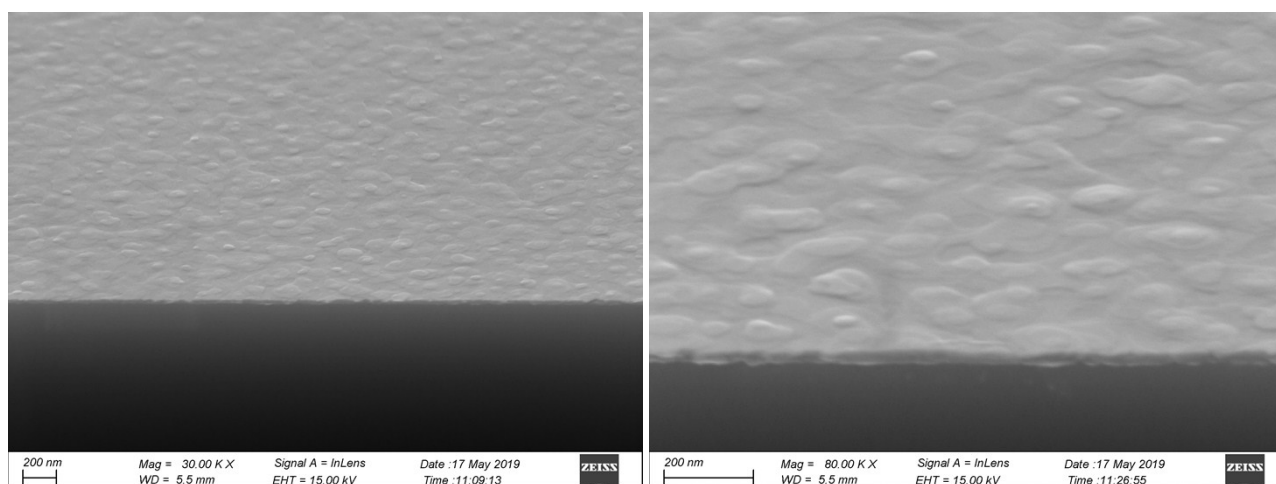


Figure S3. Tilted cross-section SEM images of Sb_2Te_3 - *Post-Growth Annealing (3)* films.

2. AFM Images

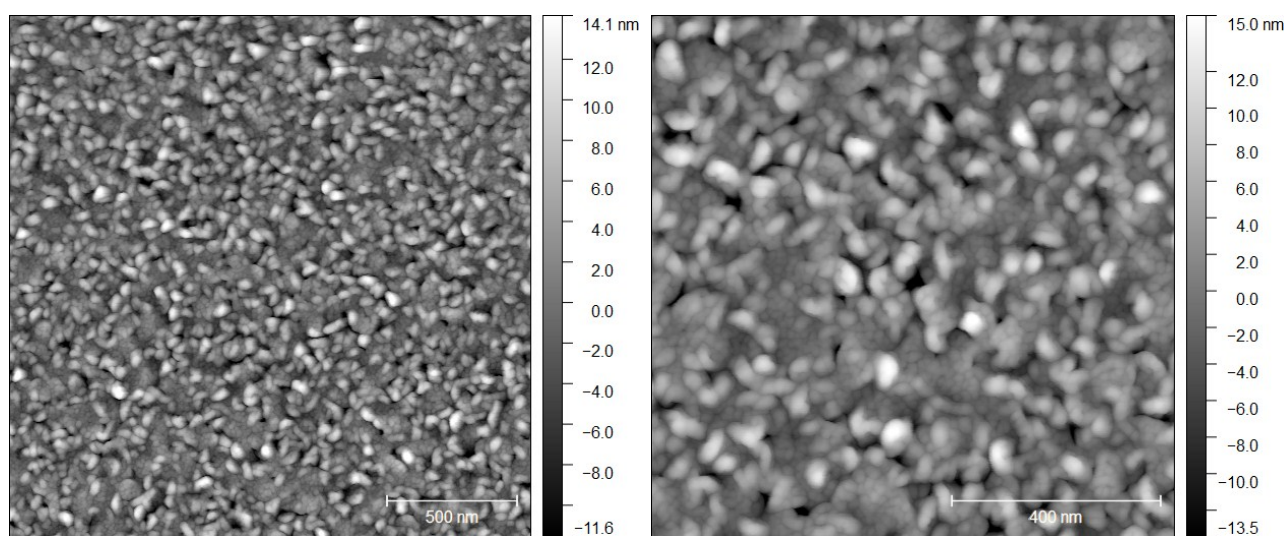


Figure S4. AFM images of Sb_2Te_3 - *As Deposited* (1) films.

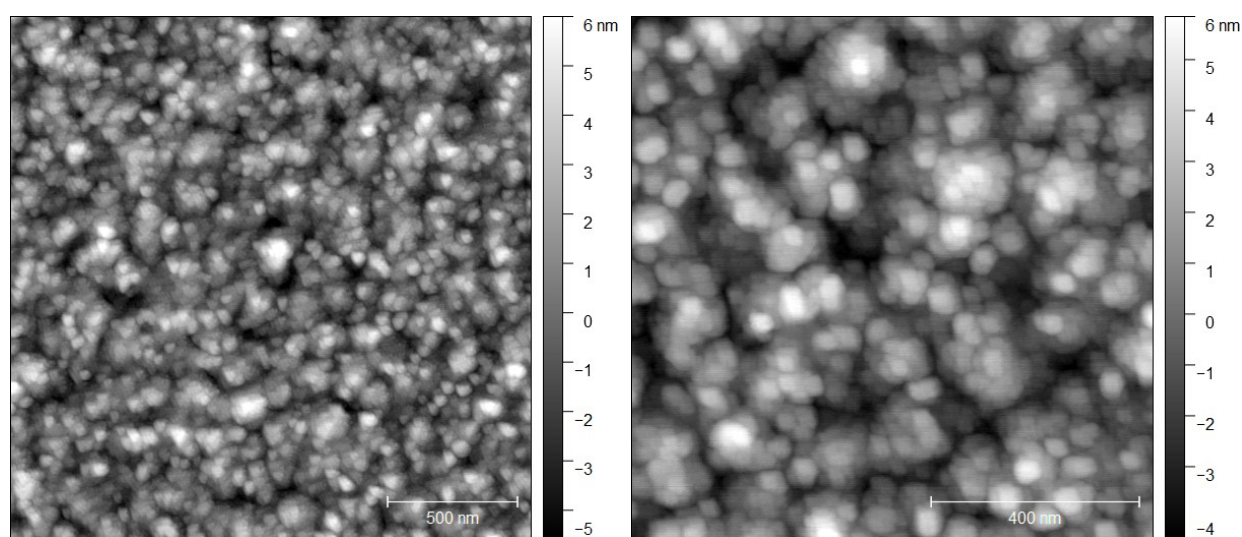


Figure S5. AFM images of Sb_2Te_3 - *Substrate Annealing* (2) films.

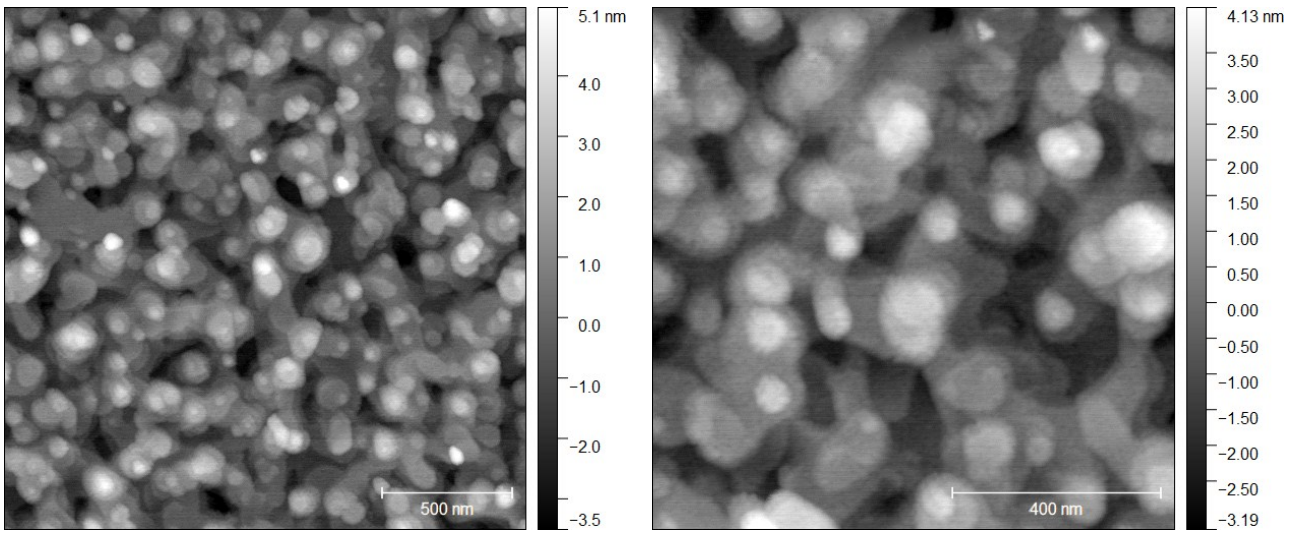


Figure S6. AFM images of Sb_2Te_3 - *Post-Growth Annealing* (3) films.

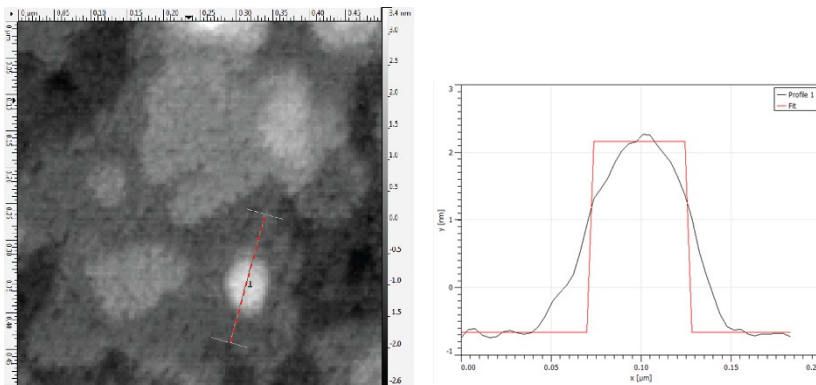


Figure S7. Selected surface profile of Sb_2Te_3 - *Post-Growth Annealing* (3); Step height: 3 nm.

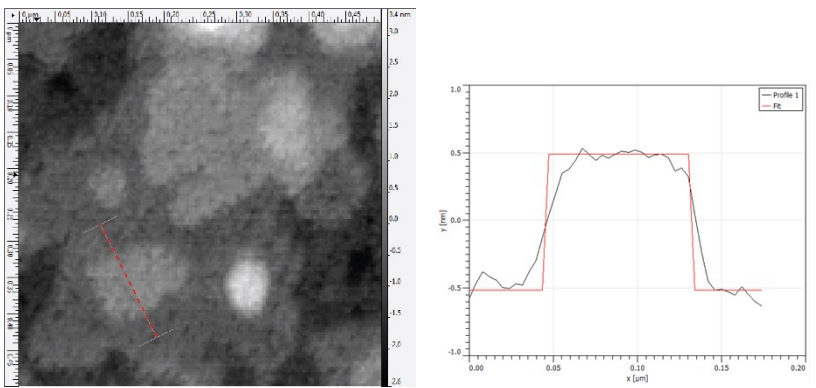


Figure S8. Selected surface profile of Sb_2Te_3 - *Post-Growth Annealing* (3); Step height: 1 nm.

3. TEM Images

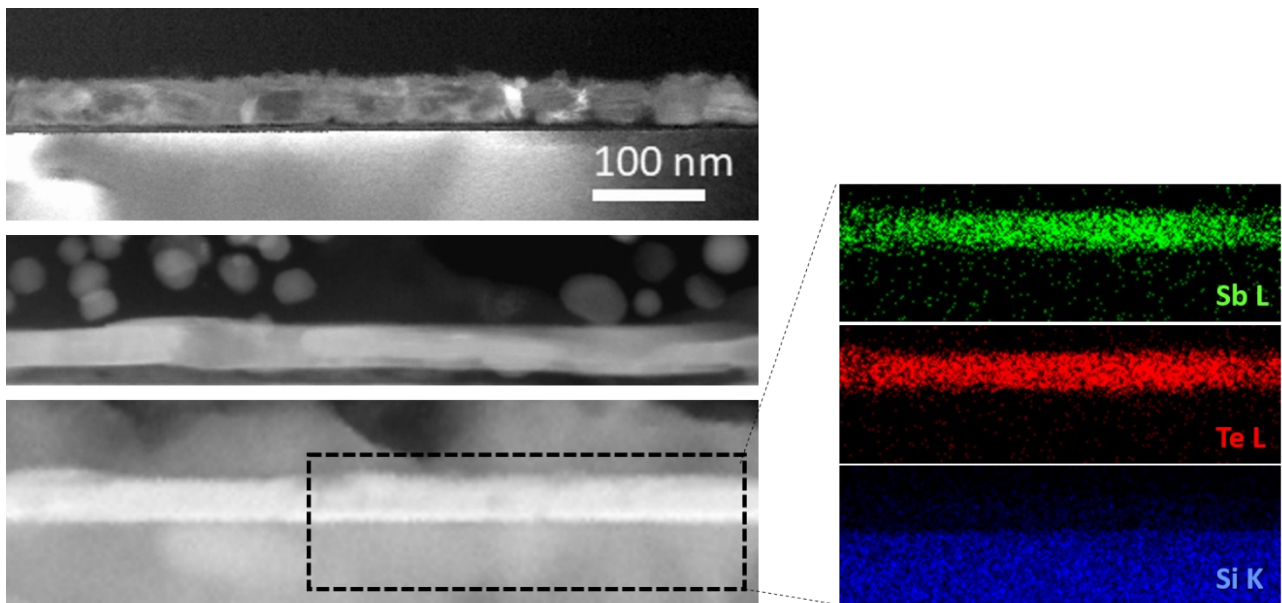


Figure S9. On the left, the STEM-HAADF images of the three different Sb_2Te_3 sample topology are reported for comparison: from the top, Sb_2Te_3 - *As Deposited* (1), Sb_2Te_3 - *Substrate Annealing* (2), and Sb_2Te_3 - *Post-Growth Annealing* (3). On the right, the EDX elemental maps obtained from the dashed square region of the sample Sb_2Te_3 - *Post-Growth Annealing* (3). Te and Sb are homogeneously distributed in the layer.

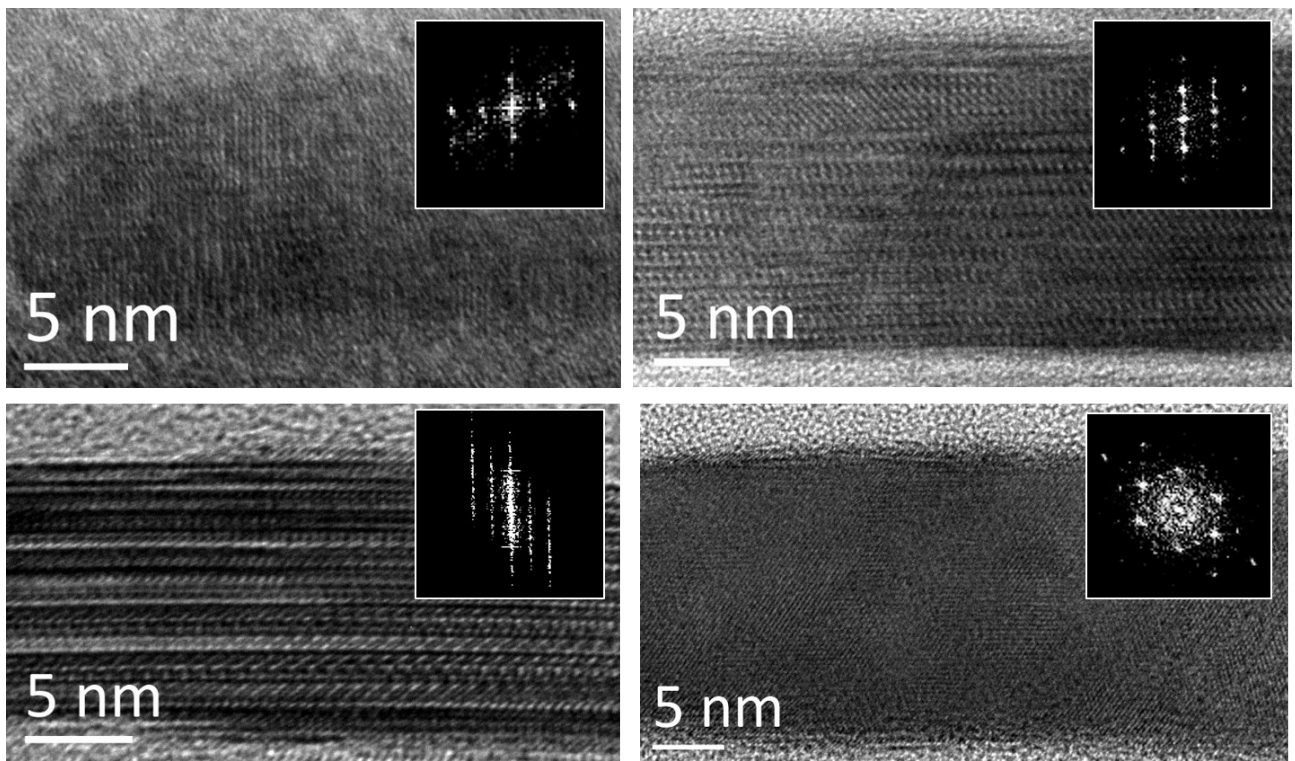


Figure S10. TEM images and related FFTs of Sb_2Te_3 - *Substrate Annealing* (2) films: examples of the variability in the crystallographic orientations of some different grains.

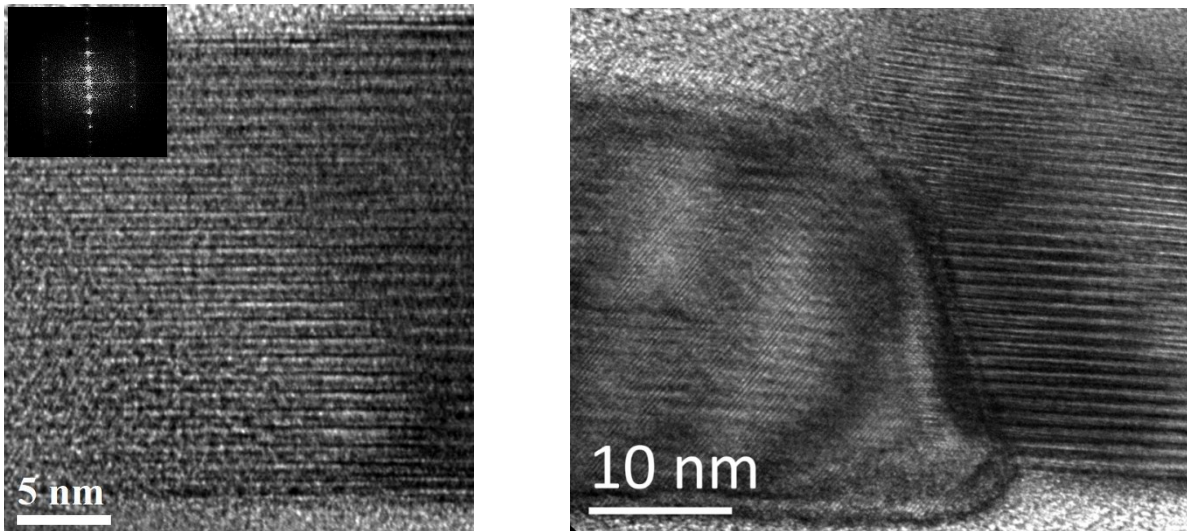


Figure S11. High resolution TEM images of Sb_2Te_3 - *Post-Growth Annealing* (3) film. Left: the quintuple stack of the Sb_2Te_3 rhombohedral crystalline structure (R -3m space group); the stacking period, measured from the FFT in the inset, is 1 nm. Right: the boundary between two grains.

4. TXRF Spectra

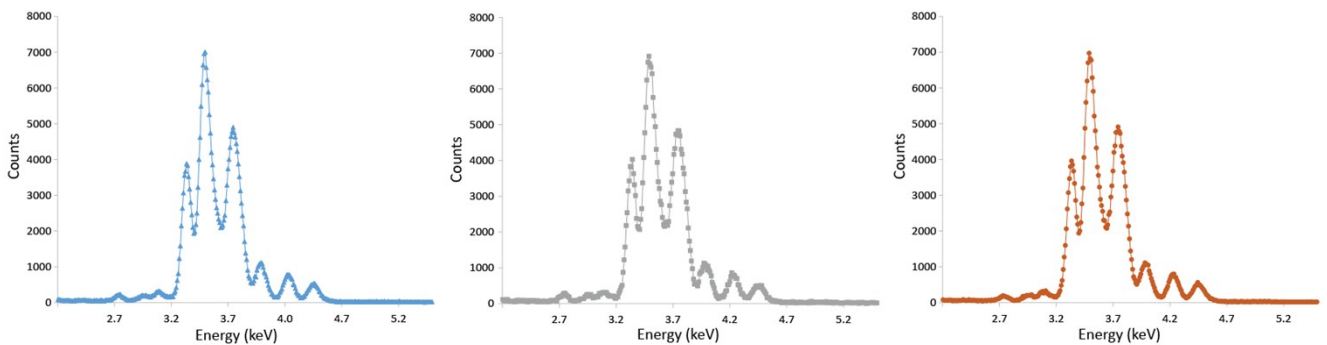


Figure S12. TXRF Spectra of Sb_2Te_3 - *As Deposited* (1) (blue, left), Sb_2Te_3 - *Substrate Annealing* (2) (grey, middle), and of Sb_2Te_3 - *Post-Growth Annealing* (3) (red, right).

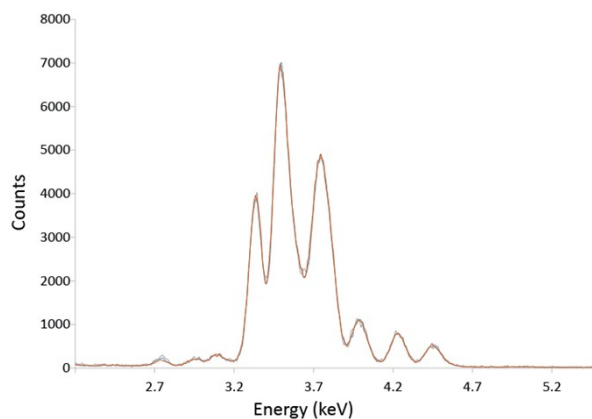


Figure S13. Overlap of the TXRF Spectra shown in Figure S12 indicating the same elemental composition in 1, 2, 3.

5. XP Spectra

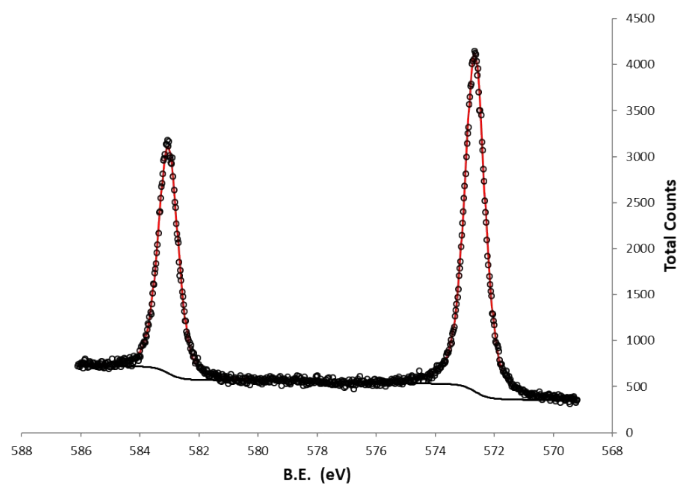


Figure S14. Te 3d XPS of Sb_2Te_3 - As Deposited (1). Te $3d_{5/2}$: 572.6 eV ($\Delta = 10.4$ eV).

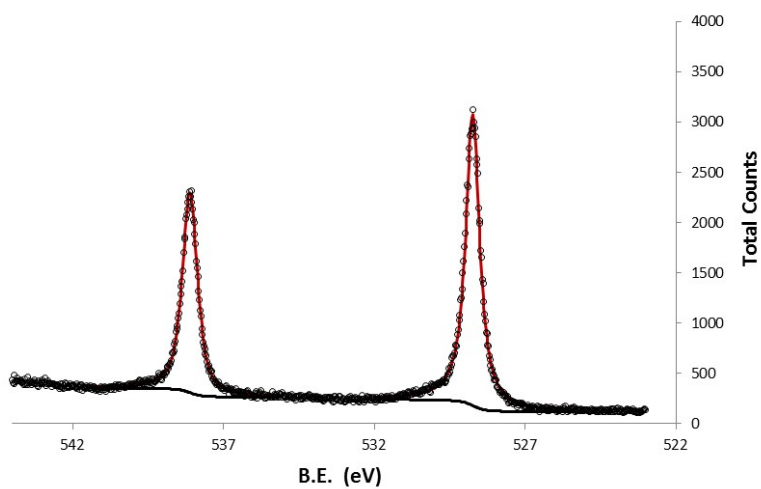


Figure S15. Sb 3d XPS of Sb_2Te_3 - As Deposited (1). Sb $3d_{5/2}$: 529.0 eV ($\Delta = 9.35$ eV).

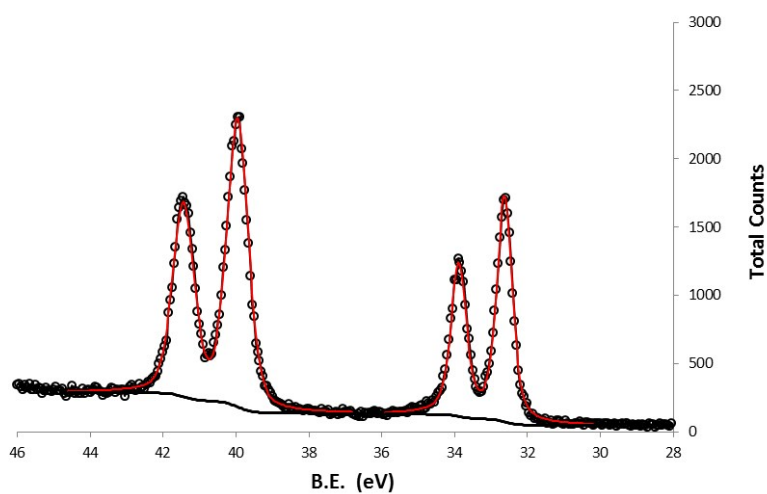


Figure S16. Te and Sb 4d XPS of Sb_2Te_3 - As Deposited (1). Te $4d_{5/2}$: 40.2 eV ($\Delta = 1.5$ eV); Sb $4d_{5/2}$: 32.9 eV, ($\Delta = 1.2$ eV).

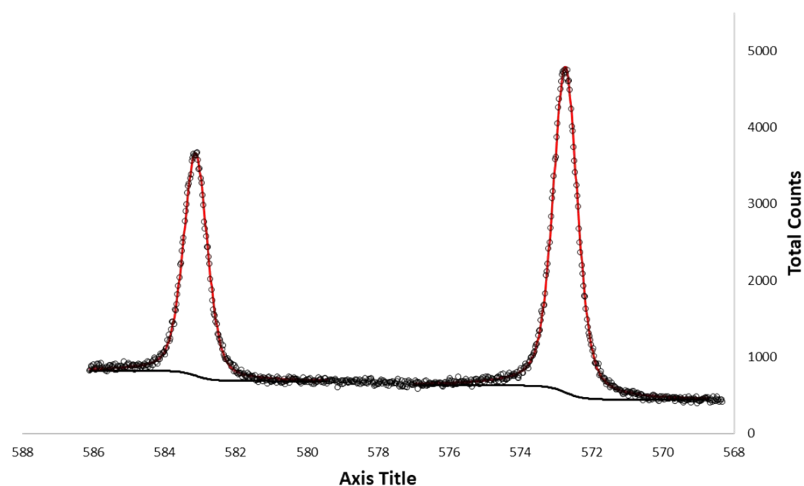


Figure S17. Te 3d XPS of Sb_2Te_3 - *Substrate Annealing* (3). Te $3d_{5/2}$: 572.7 eV ($\Delta = 10.4$ eV).

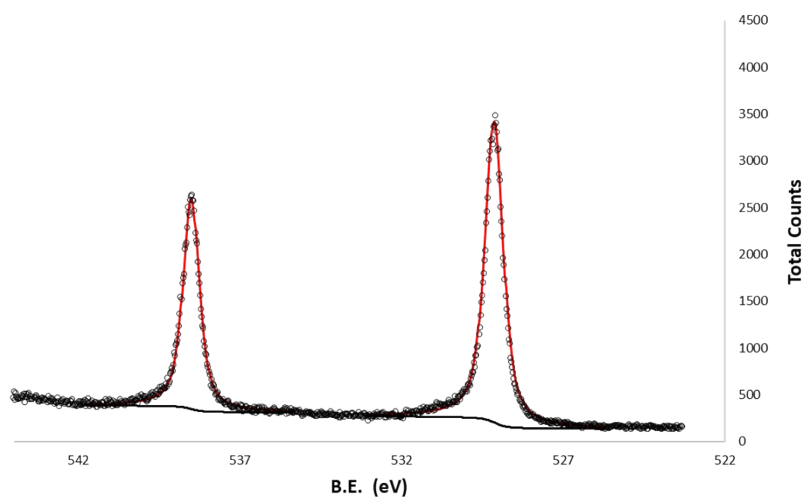


Figure S18. Sb 3d XPS of Sb_2Te_3 - *Substrate Annealing* (3). Sb $3d_{5/2}$: 529.1 eV ($\Delta = 9.4$ eV).

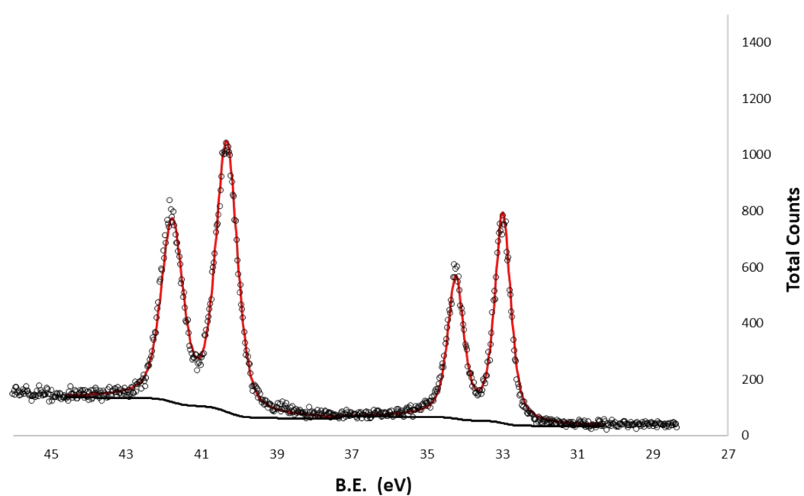


Figure S19. Te and Sb 4d XPS of Sb_2Te_3 - *Substrate Annealing* (3). Te $4d_{5/2}$: 40.3 eV ($\Delta = 1.5$ eV); Sb $4d_{5/2}$: 33.0 eV, ($\Delta = 1.3$ eV).

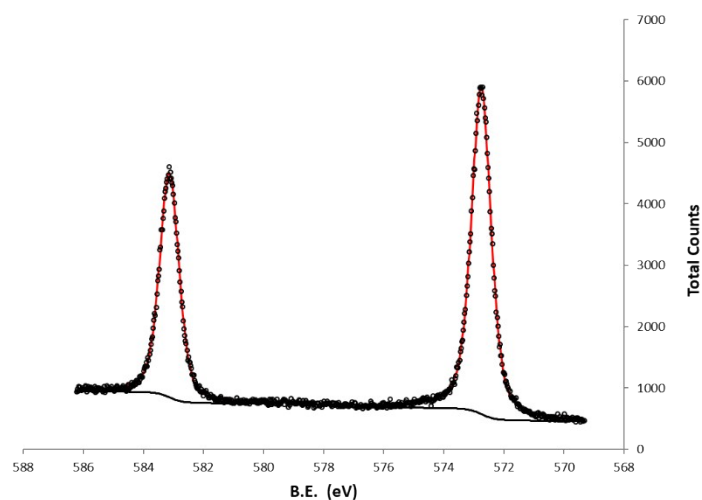


Figure S20. Te 3d XPS of Sb_2Te_3 - *Post-Growth Annealing* (3). Te $3d_{5/2}$: 572.7 eV ($\Delta = 10.4$ eV).

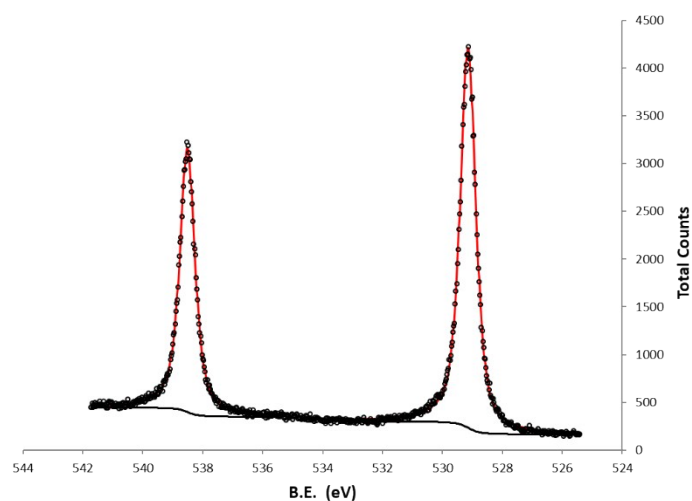


Figure S21. Sb 3d XPS of Sb_2Te_3 - *Post-Growth Annealing* (3). Sb $3d_{5/2}$: 529.1 eV ($\Delta = 9.35$ eV).

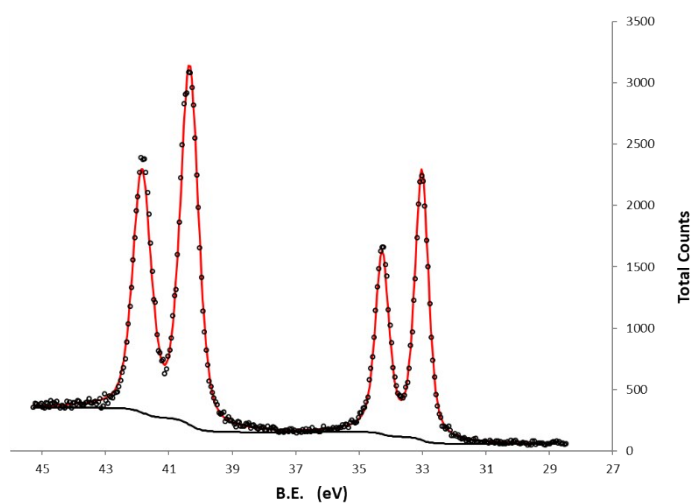


Figure S22. Te and Sb 4d XPS of Sb_2Te_3 - *Post-Growth Annealing* (3). Te $4d_{5/2}$: 40.3 eV ($\Delta = 1.5$ eV); Sb $4d_{5/2}$: 33.0 eV, ($\Delta = 1.2$ eV).

6. XRR Measurements

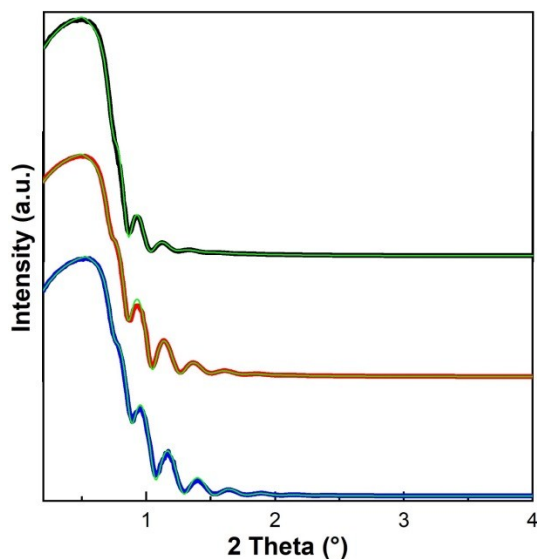


Figure S23. XRR measurements of Sb_2Te_3 - *As Deposited* (1) (black, top), Sb_2Te_3 - *Substrate Annealing* (2) (red, middle), and of Sb_2Te_3 - *Post-Growth Annealing* (3) (blue, bottom).

	Thickness (nm)	Electronic density ($\text{e}/\text{\AA}^3$)	Roughness (nm)
<i>Sb₂Te₃ - As Deposited</i>	33.7	1.75	3.1
<i>Sb₂Te₃ - Substrate Annealing</i>	32.5	1.68	2.0
<i>Sb₂Te₃ - Post-Growth Annealing</i>	32.0	1.80	1.5

Table S1. Thickness (nm), Electron density ($\text{e}/\text{\AA}^3$), and Roughness (nm) of Sb_2Te_3 - *As Deposited* (1), Sb_2Te_3 - *Substrate Annealing* (2), and of Sb_2Te_3 - *Post-Growth Annealing* (3) extracted from XRR measurements.

7. XRD Measurements

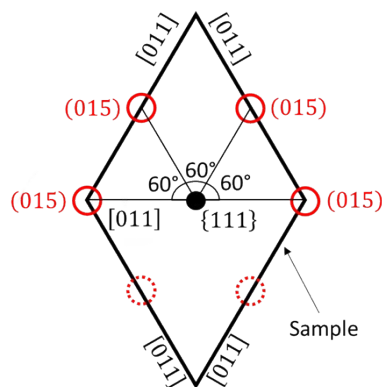


Figure S24. Schematic representation of the sample and the Sb_2Te_3 015 reflections. The solid black circle indicates the Si{111} out-of-plane orientation of the substrate. The position of the reflections from the Sb_2Te_3 (015) planes (red circles) with respect the [011] planes of the Si{111} substrate forms an angle of 60° . The latter condition can be easily associated to a single family of Sb_2Te_3 hexagonal crystalline structures with a fixed orientation in the film plane.